Science of the Total Environment 906 (2024) 167647

Contents lists available at ScienceDirect

Science of the Total Environment

journal homepage: www.elsevier.com/locate/scitotenv

Understanding the spatial variation in lithium concentration of high Andean Salars using diagnostic factors

Jafar Al-Jawad *, Jonathan Ford, Evi Petavratzi, Andrew Hughes

British Geological Survey, Keyworth, Nottinghamshire NG12 5GG, UK

HIGHLIGHTS

- Environmental linkage of lithium evolution over high Andean salars not yet identified
- Ore deposit model using weather and basins' characteristic parameters employed
- Normalising lithium by parameters successfully produced environmental correlations.
- Atacama spatially is an outlier, and small salars may have high lithium concentration.
- Lithium concentration level is not a matter of basin size.

GRAPHICAL ABSTRACT

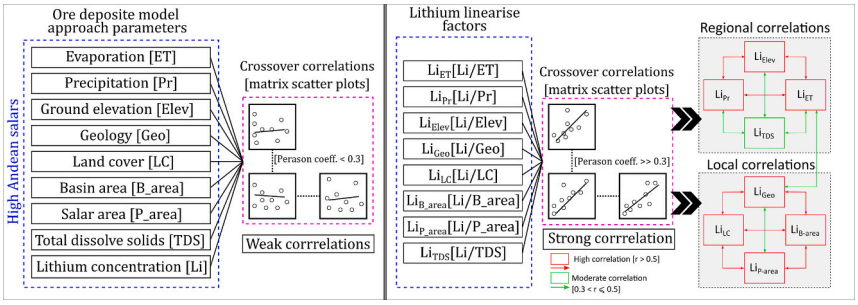

ARTICLE INFO

Editor: Christian Herrera

Keywords:
Lithium Triangle
Brine
Deposit model
Normalised lithium
Volcanic rocks

ABSTRACT

Salars (basins of internal drainage) in the "Lithium Triangle" countries (Argentina, Bolivia, Chile) hold >50 % of the global lithium resources within lithium-rich brines. Given the imperative for lithium production to enable the energy transition and that salars by their very nature are highly variable, so a framework to both characterise their differences as well as identifying their similarities would be beneficial to understanding their provenance and potential for exploitation.

In this study, data for 29 salars based on environmental factors: rainfall, evaporation as well as their physical characteristic: pan size and basin size have been used to characterise them along with those describing their setting land-use/cover and geological outcrop. These parameters have been normalised by creating a ratio of the lithium concentration divided by the factor for each salar. Cross-correlation has been used to develop relationships between these normalised factors, combined with principal component analysis to identify clustering and to further characterise groupings of behaviours.

Two such relationships emerge out of this process: regional and local. Regional covers factors such as elevation, precipitation, and evaporation; local includes size of watershed, salar nucleus, land cover and geological outcrop in the watershed. However, Salar de Atacama is identified as an outlier and so the transferability of the understanding of its provenance and operation must be treated with caution. Other salars could be added to the framework as more information becomes available. The methodology presented here could help exploration by characterising salars into categories as their smaller size may not necessarily mean lower lithium mass. Further, such a framework can inform policy decisions and instruments by recognising the complexity of salars combined with the need to understand the environmental impacts of brine extraction.

* Corresponding author.
E-mail address: jafar@bgs.ac.uk (J. Al-Jawad).

https://doi.org/10.1016/j.scitotenv.2023.167647
Received 5 June 2023; Received in revised form 12 September 2023; Accepted 5 October 2023
Available online 12 October 2023

1. Introduction

Lithium brine resources in the "Lithium Triangle" (Argentina, Bolivia, Chile) in South America are vast and located in salars (basins of internal drainage). The salars in the "Lithium Triangle" countries hold >50 % of the global lithium resources (Munk et al., 2016). The time-window for bringing lithium production to market is soberingly short. Projections suggest that lithium demand for clean energy technologies is growing faster than other major minerals, primarily due to the move towards electrification in transport. According to the International Energy Agency, lithium demand is expected to increase by over 40 times by 2040 (IEA, 2021). To ensure that the increase in supply of lithium can be met within this timescale, an overall understanding of lithium brine resources is needed. Given the number and variety of salars then methods by which they can be assessed and compared within the "Lithium Triangle" are required.

High Andean salars are some of the most complex groundwater systems in the world, combining atmospheric interactions (rainfall patterns), the hydrosphere (groundwater and surface water) and the lithosphere (lithium release and transport from rocks) along with solute concentration by evaporation (Corenthal et al., 2016). They represent basins of internal drainage, so-called "endorheic" basins, at elevations of over 2300 m above sea level (m.a.s.l), often higher and exhibit low rainfall and high evaporation rates (Munk et al., 2018). The salars, typically, are sited in basinal settings surrounded by volcanic deposits that are the source of mineralised lithium (e.g. andesite, tuff), which are leached into the salars by the movement of surface waters and groundwater (Rossi et al., 2022). The process of leaching solutes and transporting them to the salars can take of the order of 100,000 s years (e.g., Atacama; Corenthal et al. (2016)). The salars themselves comprise sedimentary deposits ranging from clays, silts, sands and various evaporite minerals through to halite, NaCl. They are formed within a highly active system geologically, which has changed significantly over the last few million years, e.g. Salisbury et al. (2011). The salars typically have a central area or nucleus in which the brines are created by evaporative processes and, typically, this is where the greatest concentration of lithium is located.

Rainfall is typically very low on the salars, of the order of 10s mm/annum, but rising to 150–200 mm/annum as the elevation increases away from the salar itself e.g. Atacama (Marazuela et al., 2018). Rainfall recharge is, therefore, very limited, if it occurs at all in the nucleus. Surface water and groundwater inflows to the salars, whilst small, are significant to maintain the fresh/brackish surface water systems. Periodic flooding by surface waters helps maintain the water balance, sporadically in Atacama (Boutt et al., 2016) and more regularly in wetter salars such as Salar de Uyuni, Bolivia (Petavratzi et al., 2022a). Outflows are primarily from evaporation, which is orders of magnitude higher than the rainfall and abstraction. The latter can take place for potable water supply, industrial supply or brine extraction itself. Climate change, likely to result in an increase in temperature but forecast to produce variable impacts on rainfall, will change the balance of inflows and outflows over time (Oyarzún and Oyarzún, 2011).

Typically, the brines are super-saturated and have densities of around 1208 kg/m^3, which is significantly higher than sea water (1030 kg/m^3). For the brine solute mass, NaCl is the main constituent with trace elements of metals such as K, Mg, and Li. These accumulate over very long time periods as crust-forming evaporites and also in solution in brines (Houston et al., 2011). A series of chemical reactions and precipitation processes take place that result to the brine chemistry evolving over time and over the nucleus (exhibiting a spatio-temporal dimension) (Hamman et al., 2015).

No two salars are alike, although some fundamental similarities exist. Salars are often classified as mature halite salars and immature clastic salars (Houston et al., 2011). Mature salars are characterised by a relatively uniform and thick sequence of halite deposited under subaqueous to subaerial conditions. Immature salars are often characterised by higher precipitation, lower evaporation and tend to be at higher elevation towards the wetter northern and eastern parts of the region (Houston and Hartley, 2003). For mature salars with a saturated brine then the outflow is via evaporation mainly from surface water ponds around the margin and from the centre of the salar (nucleus) itself. Evaporation has an exponential decreasing relationship with depth to the water table (Houston, 2006a). This means that once the water table is 0.5 m below the salar surface then evaporation reduces markedly (Marazuela et al., 2020). Potential evaporation is also controlled by the salinity of the water being evaporated, with the magnitude decreasing with increasing brine concentration (Houston, 2006b). Considerable time is required for lithium to accumulate, a process which requires a suitable source of lithium and the mechanism to transport the lithium to the salar itself. Once in the salar then evaporative processes concentrate the lithium by removing water and retaining the solute mass (Munk et al., 2018).

Common regional and local characteristics (or parameters) of Li-rich brine have been identified by Bradley et al. (2013) using an ore deposit model approach: (1) arid climate; (2) closed basin containing a playa or salar; (3) tectonically driven subsidence; (4) associated igneous or geothermal activity; (5) suitable lithium source-rocks; (6) one or more adequate aquifers; and (7) sufficient time to concentrate a brine. It is likely, a combination of these parameters may represent the lithium evolution environment within the basin. Excluding (6), Munk et al. (2016) elaborates how these parameters may be implemented to help lithium ore exploration features on a global scale. They present and discuss eighteen basins that share these parameters, however how each of these characteristics are correlated with respect to lithium evolution has not yet been fully explored (Munk et al., 2016), accordingly variation in the spatial regional lithium concentrations pattern have not been fully developed (López Steinmetz et al., 2020). An example of such a case is the significant variation of lithium concentration between the Salar de Atacama and Salar de Guayatayoc with Li ≈ 1400 and ≈100 mg/l, respectively (López Steinmetz et al., 2020). Further details of Salar de Atacama and Uyuni can be found in the supplementary material (S1).

.As stated above, a regional context is required to understand the variability in salars, one of the first attempt at collating regional data for salars was undertaken by Risacher and Fritz (1991) for Bolivian salars, where they collated and examined geochemical data for 30 salars. Their work showed the importance of leaching of volcanic rocks by meteoric (rainfall) waters and hydrothermal processes as well as leaching of ancient evaporites. They extended their work (Risacher and Fritz, 2009) to cover both Bolivian and Chilean salars – 84 in total. This work confirmed different sources of lithium in the basins: hydrothermal and re-working of halite deposits and they proposed that source rocks combined with a semi-arid climate are an important part of the lithium concentration process. In comparing salars from different countries within Lithium Triangle they showed that inflows to the salars are three-times more concentrated in Chile than Bolivia and that the waters are enriched with respect to sulfate salts. This leads to sulfate-rich brines being formed in Chilean salars whilst Bolivian salars tend to be calcium-rich. However, the source of the samples was different for each country; Bolivian samples were from surface waters and the Chilean one from groundwaters using boreholes to provide the samples.

The work undertaken for Bolivian and Chilean salars has been complemented by López Steinmetz et al. (2020) who collated and examined geochemistry for 12 salars in northern Argentina. Their work tried to correlate lithium concentration with Total Dissolved Solids (TDS) but was unable to find a suitable relationship. However, they concluded that the size of salar is linked to lithium concentration, particularly once the larger salars have been taken out. The work was extended by López Steinmetz and Salvi (2021) who examined geochemistry for 49 salars. They confirmed that the larger and more mature the salar resulted in higher lithium concentration, but that there was limited spatial correlation with respect to elevation as all the salars are located at high elevations. For instance, they demonstrated a linear

relationship between the pan size and lithium concentration and showed that the mean lithium concentration in a salar is roughly half the maximum lithium concentration.

To date, there has been limited work to identify possible correlations (e.g., similarities and outliers) in salars' system considering the deposit model parameters mentioned by Bradley et al. (2013) and Munk et al. (2016), have been reported in the literature. Here, regional correlations of 29 salars are examined based on a deposit model and is used to identify anomalies in the salars within the Lithium Triangle, to further understand a series of questions: (1) Why do apparently similar salars have different lithium concentrations? (2) What is/are the driving parameter/parameters for this variation in lithium concentration? (3) How can this help understand the processes to determine lithium evolution and the potential source rocks? Addressing these questions will enable studies of individual salars to be placed into context for further insight as well as the understanding of lithium brine formation and evolution processes.

2. Material and methods

2.1. Study area

2.1.1. Location and topography

Characterised by multiple high-altitude endorheic drainage basins, the Lithium Triangle ranges from hyper-arid Atacama Desert in the west, Bolivian Altiplano in the north and the Puna landscapes of Argentina in the south and east (Fig. 1a). It represents the most extensive area of high plateaus on Earth outside of the Tibetan Plateau. The descriptive terms Altiplano and Puna are often interchangeable.

The topography of the region is dominated by very high mountains (Fig. 1b), mainly of volcanic origin, cordillera (mountain ridges), plateaux and internal drainage basins, many of which are characterised by bofedales, high altitude peatlands, as well as salars. The volcanoes in the region are the highest on Earth (e.g., Llullaillaco 6739 m; Ojos del Salado, 6893 m) and may be either active, dormant, or extinct. This high incidence of volcanism, with weathering into endorheic drainages, gives rise to the accumulation of lithium-rich brines within these salar systems (Meixner et al., 2021).

The area has a spatially consistent hydrology in that these are arid and semi-arid areas consisting of fragile ecosystems which are vulnerable to environmental change (human intervention and climate change). However, there are differences for each country based on climatic variation. Rainfall is controlled by orographic processes due to the extreme changes in relief (~kms) as well as the prevailing wind direction (north to south) (Houston and Hartley, 2003).

2.1.2. Climate

The Puna region is defined by its dry continental climate where rainfall is scarce (between 200 and 500 mm per year) (Houston and Hartley, 2003), winds are frequent and of variable intensity, temperatures are predominantly cool or cold all year round, the thermal oscillation is very large, between 25 and 40 °C between the coldest month and the warmest (Brêda et al., 2020). There are several months with very harsh winters that contrast with very hot summers. The daily thermal oscillation is also often high that defines the severity of the environment. This environmental dryness is accentuated by strong solar radiation.

The scarce precipitation occurs mainly in the austral summer (November to February) and can be of great intensity. This can be in the form of snow or hail in the highest mountain ranges, while at a lower altitude rainfall of greater total magnitude tend to occur (Houston, 2006b). In Fig. 1c, the spatial distribution of mean annual precipitation in the High Andes region is evident, and clearly shows salars and their associated basins receive different rainfall rates. Example of rain variation can be found in the supplementary data (S2).

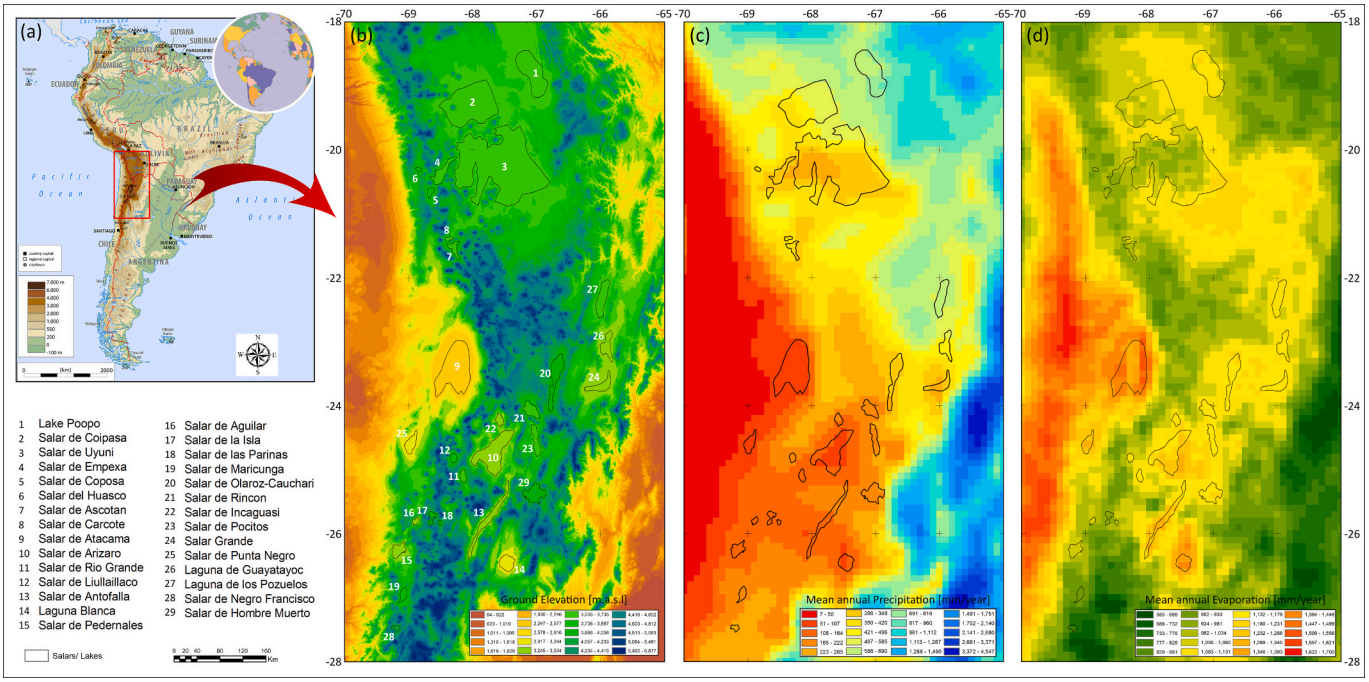

Fig. 1. (a) Location map of High Andes in South America (red rectangle) [adopted from (WorldAtlas, 2020)]. (b) Ground elevation [m.a.s.l], derived from 30 M Digital Elevation Model (DEM) of Shuttle Radar Topography Mission (SRTM) (Farr et al., 2007), and pan salt location of 29 selected Salars in High Andes region which ranged from about 2500 to 6800 m.a.s.l. (c) Mean annual precipitation [mm/annum], derived from ERA5-Land hourly developed by Copernicus Climate Change Service (C3S) at ECMWF (Muñoz-Sabater et al., 2021), ranged from about 7 mm in eastern side to about 4500 mm in south-western side. It shows how rainfall patterns changed over the region, hence salars received different direct recharge rate that may affect lithium evolution over salars. (d) Mean annual evaporation rate [mm/annum], derived from Penman formulation (Penman, 1948, 1963; Valiantzas, 2006) that rely on surface parameters such as wind speed, temperature, surface solar radiation, etc. ranged from about 580 to about 1700 mm in south-western and eastern side, respectively, which may partially explain spatial lithium concentration variation.

Evaporation from any salar is a core feature of the brine evolution cycle, as in Fig. 1d. For this paper, we focus on evaporation from open-water bodies from the nucleus of the salar and areas of open water such as lagunas. Salar de Atacama and Salar de Punta Negro are located within the area of highest evaporation rate in the western side of the Andes (>1300 mm/annum), which coincides with the very low rainfall rate in eastern part of the study area (Fig. 1c). The mean evaporation rate for Salar de Uyuni is approximately 850 mm/annum but increases to the south to approximately 1200 mm/annum (see Fig. 1c). In addition, the nature of the significant area of white salt pan possibly increases the uncertainties in surface parameters such as solar radiation and heat flux.

2.1.3. Hydrology

The water cycle/balance in any basin including salars is controlled by many parameters such as catchment area size, soil texture, land cover type, etc. captures lithium evolution and concentration. In general, large watershed size capture more water from rainfall, which theoretically refer to larger total recharge volumes than smaller basins, however other parameters such as rainfall and evaporation patterns spatial variation, soil infiltration rates, land vegetation extend may or may not affect this. To explore basin size and its influence on lithium evolution, open data watershed boundaries adopted from HydroSHEDS (Lehner et al., 2008). HydroSHEDS is a "mapping product that provides hydrographic information for regional and global-scale applications in a consistent format" (see https://www.hydrosheds.org/) (Fig. 2a). Here, some major basin's salars extend beyond the selected study area border, such as Lake Poopo and Salar de Coipasa, but the full basin area considered for calculations. When two salars share a watershed, then the area of the watershed is equally distributed between each salar watershed.

2.1.4. Geology

Geological formation has been adopted from open data geological map of South America (Gómez et al., 2019) with scale 1:5 M, (https://www2.sgc.gov.co/MGC/Paginas/gmsa5M2019.aspx), as in Fig. 2b. Although of small-scale, the data provides sufficient geological details to cover rock types and formation ages. To investigate the formations that are likely to participate in lithium evolution, we reclassified the map based on rock types, as in Fig. 2c and the background geology is described for each Lithium Triangle country as follows:

Background: The Andes are a relatively young (20–30 Ma) mountain range. They were formed by uplift processes resulting from tectonic plate movements bordering the Pacific coast of South America. During the volcanically active phase, ash deposits such as Ignimbrites were deposited on the landscape resulting from pyroclastic flows (Meixner et al., 2021). These deposits were derived from magma with varying chemistry, resulting in variation of lithium concentration in the rock mass.

Lithium-bearing salars form through a combination of geological, hydrological, and meteorological process: lithium is leached from suitable country rocks in inland drainage basins and transported in solution by rivers and groundwater into lower-lying areas. Here, evaporation greatly exceeds precipitation, hence water is lost through evaporation and Li and other elements are gradually precipitated in the form of rock salt ('halite') and related evaporite-minerals or, in the case of Li, concentrated into a residual brine (Houston et al., 2011). More details of the geological setting on a country basis can be found in the supplementary materials (S3).

2.1.5. Land cover

Land cover is an important parameter as it has direct impact on runoff from topographics high to lower-lying parts of the basin, e.g., salt pan. Increased vegetation cover like grass which could result in slowing the flow of runoff, which could reduce modify recharge processes to the salt pan. Basins with more bare areas likely receives more direct recharge from runoff that may improve lithium concentration, such as in Salar de Uyuni (Risacher and Fritz, 1991) where high lithium

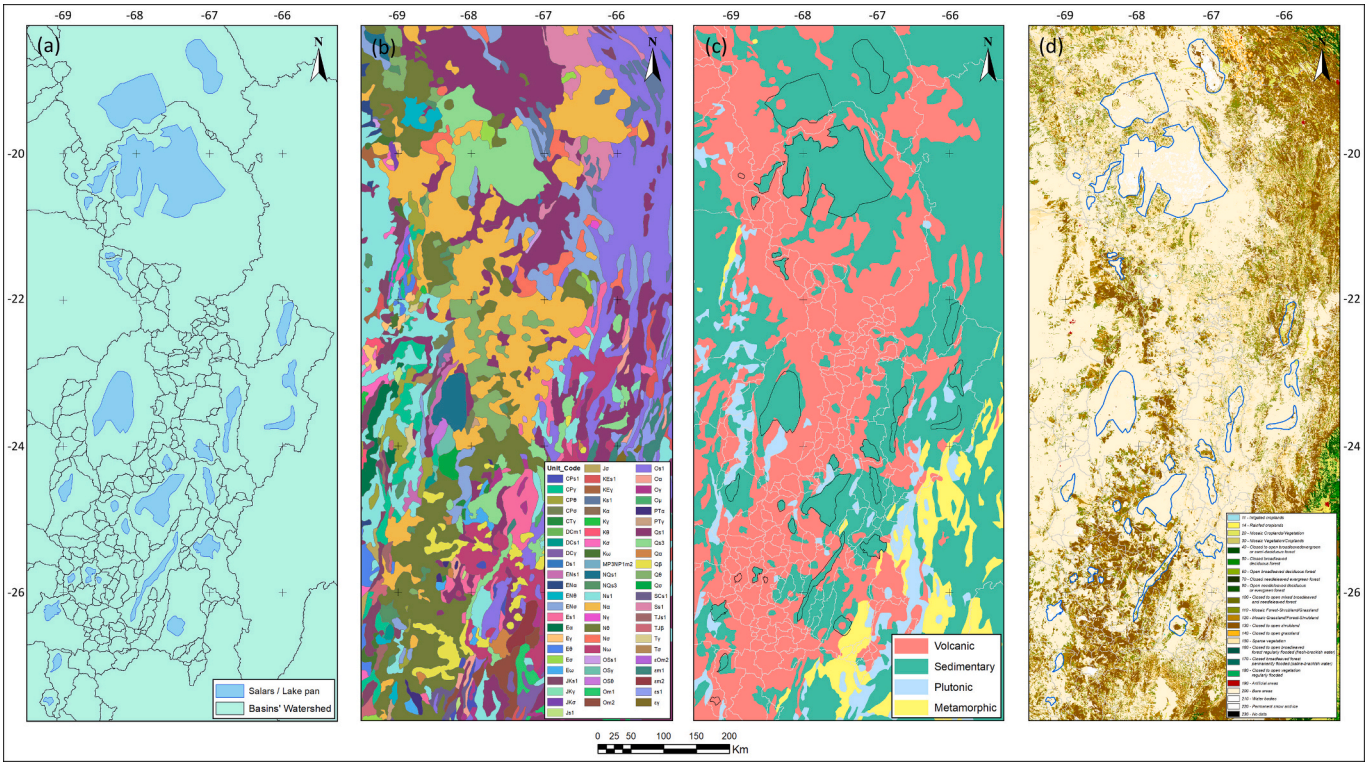

Fig. 2. Basin Characteristics as (a) illustrates regional basins' watershed boundaries adopted from HydroSHEDS (Lehner et al., 2008); (b) regional geological map adopted from Gómez et al. (2019) shows detail geological units; (c) classified regional geological map based on rock types; and (d) regional land cover types adopted from (GlobCover., 2009).

concentration located at surface water drainage in the salar's southern part. Additionally, the evaporation rate increase when groundwater level approaches the surface level, in turn increasing the brine concentration under salt crust pan (Houston, 2006a). Fig. 2d illustrates land cover types adopted from Land cover, Central and South America (GlobCover., 2009), with spatial Resolution of 0.3 km. details in (https://databasin.org/datasets/693f573b98834d1cbcc364e7f0b8e5db/). The Land cover classes defined in harmony with the United Nations (UN) Land Cover Classification System (LCCS). The figure shows high Andes region is mainly covered by "Closed to open Shrubland" and "Mosaic Grassland/Forest-Shrubland" types, with small areas with "Mosaic Forest-Shrubland/Grassland", other zones mainly bare areas. Dense vegetations such as broadleaved and needle leaved forest located in the south-east and north-east part of the study area, which correspond to high rainfall rates (see Fig. 1c).

2.1.6. Geochemistry

Total Dissolved Solids (TDS), represents the dissolved ions of salts, minerals, and metals that can be found in natural waters, this parameter has been adopted widely for various correlations at local and region scale (López Steinmetz and Salvi, 2021; López Steinmetz et al., 2018; López Steinmetz et al., 2020; Risacher et al., 2003; Risacher and Fritz, 2009; Rissmann et al., 2015). It ranged from 20 g/l in Salar de Coposa, to 247 g/l in Salar de Rio Grande with mean and standard deviation about 119 and 69 g/l, respectively, in which 12 salars with TDS < 100 g/l, and 13 in range of 100–200 g/l, while only 5 salars exhibit TDS > 200 g/l.

The distribution of lithium concentration in salars is discussed in more detail below, but a summary is provided for completeness. Regional lithium concentration varies between 16 mg/l in Salar de Coposa, and 1000 mg/l in Salar de Atacama, with mean of approximately 336 mg/l and standard deviation of 238 mg/l. As mentioned previously, the reasons for the distribution of lithium concentrations are not well defined, but it can be classified by their Li [mg/l] range as: (1) Li < 100; (2) $100 \leq$ Li < 500; and (3) Li ≥ 500, in which (1) 5 salars (2) 19 salars; and (3) 5 salars, respectively. Noticeably, the lithium concentration of most salars is within class (2), in which 3 salars are in the 100–200 mg/l sub-class, 12 salars are within the range of 200–400 mg/l sub-class and 4 salars are within the 400–500 mg/l sub-class. However, more detailed investigations and sampling (also at greater depth) is required to enhance existing figures as most of the existing Li values are based on shallow sampling, like in López Steinmetz et al. (2020) and Risacher and Fritz (2009).

2.2. Framework

2.2.1. Diagnostic parameters

The use of a deposit model to characterise lithium occurrence within salars and associated parameters have been proposed by Bradley et al. (2013) and Munk et al. (2016). Their work is extended here and are based on data availability as presented in Table 1. Details of data calculation, manipulation and analysis of Table 1 is presented below, and relevant parameters values are provided in Table 2. Further details on the data and its processing can be found in the supplementary material.

Whilst the majority of the parameters are available directly from data sources, the exception is evaporation and the various methods of calculation are described as follows. The Penman formula for open water evaporation (Penman, 1948, 1956, 1963; Valiantzas, 2006) is as follows:

$$E_0 = \frac{\Delta . R_n}{\lambda(\Delta + \gamma)} + \frac{6.43 . E_a . \gamma}{\lambda(\Delta + \gamma)} \quad (1)$$

where R_n is net radiation at the surface [MJ/m^2/d], Δ is the slope of the saturation vapor pressure curve (kPa/°C), γ is psychrometric coefficient (kPa/°C), λ is latent heat of vaporization (MJ/kg), and E_a equal to $f_U . D$, f_U is wind function and equal to $a_U + b_U . u$, where a_U and b_U are wind function coefficients (for the original Penman equation (Penman, 1948, 1963) $a_U = 1$, $b_U = 0.536$), u is the wind velocity, $D = (e_s - e_a)$ is vapor pressure deficit (kPa); e_s is saturation vapor pressure (kPa); e_a is actual vapor pressure (kPa).

Table 1
Diagnostic key-parameters in Lithium Triangle in South America.

Parameters	Source
Topography	Salt pan elevation adopted from DEM merged maps, Fig. 1b
Climate	a) Precipitation: Salt pan mean annual precipitation rate adopted from ERA5-Land simulation data, Fig. 1c using GIS spatial tool. b) Evaporation: Salt pan open water evaporation estimated from Penmen evaporation eq. (ET) using ***pyeto*** and ***evaplib*** python packages, Fig. 1d using GIS spatial tool.
Closed basin containing a playa or salar	Salt pan area digitized from Google earth map (GoogleEarthPro, 2022), Fig. 2a
Basin characteristics	Watershed (Basin) area adopted from HydroSHEDs digital simulation, Fig. 2a
Igneous or geothermal activity and suitable lithium source-rocks	Volcanic formation area within each salar's watershed, Fig. 2c using GIS Tabulated area tool
Soil texture	Bare land cover area within each salar's watershed manipulated based on land cover map, Fig. 2d using GIS Tabulated area tool
Geochemistry	a) Salar's lithium concentration adopted from López Steinmetz and Salvi (2021) b) Total Dissolved Solids (TDS) concentration adopted from (Doran et al., 2010; GHD, 2019; López Steinmetz and Salvi, 2021; Murray et al., 2019), and mean values of adjacent basins for few missing data.

To complement the open water calculation, regional evapotranspiration using multiple methods were calculated: Penman Monteith (Allen et al., 1998), Makkink (De Bruin, 1987) Priestley – Taylor (Priestley and Taylor, 1972), and Hargreaves (Hargreaves and Samani, 1985). This was undertaken to explore the sensitivity and validity of E_0 in Eq. (1), are available in Fig. S.1(a), (b), (c), and (d) (Supplementary data). It shows that spatial patterns and values are harmonic in Penman Monteith reference (a), Priestley – Taylor (b), and Hargreaves (c) models, with maximum values exceeds 1500 mm/annum, while Makkink (d) have about 500 mm/annum, as Makkink formula express evapotranspiration of well-watered short grass in summer time (De Bruin, 1987), which are likely not to be applicable in arid climates.

The following tools were used to manipulate the aforementioned dataset to calculate target parameters such as mean annual evaporation and precipitation:

1. Climate Data Operators package (CDO) (Schulzweida, 2020): is "a collection of command line Operators to manipulate and analyse Climate and NWP model Data" like GRIB 1/2, NetCDF 3/4 file format (NWP = Numerical Weather Prediction Model), and contains >600 operators. More information can be found in (https://code.mpimet.mpg.de/projects/cdo).
2. PyEto (Richards, 2015) is a Python library to estimate reference evapotranspiration (ET_o) and to estimate other relevant meteorological data. Details in (https://github.com/woodcrafty/PyETo). The library developed to estimate ET_o over three methods: FAO-56 Penman-Monteith (Allen et al., 1998); Hargreaves (Hargreaves and Samani, 1985); and Thornthwaite (Thornthwaite, 1948).
3. Meteorology and Evaporation Function Modules for Python (Haran, 2015) is a Python library contain two packages: meteolib.py and evaplib.py. meteolib.py developed to estimate: specific heat; slope of vapor pressure curve; saturation vapor pressures; actual vapor pressures; psychrometric constant; latent heat of vaporization;

Table 2
Key-parameters values of selected salars in High Andes. These parameters were used to correlate and identify similarities, and outliers in the region. Data sources as in the table footnote.

Name	Pan area[1] (km2)	Elevation[2] (m.a.s.l)	Pr[3] (mm/y)	ET[4] (mm/y)	Basin area[5] (km^2)	TDS[6] (g/l)	Land cover[7] (km^2)	Volc. Area[8] (km^2)	Li[6] (mg/l)
Argentina									
Salar de Antofalla	865.21	3325.00	158.86	804.00	5871.50	73.00	3281.79	2364.02	209.00
Laguna Blanca	500.07	3005.00	106.20	907.04	6453.60	23.00[b]	4730.82	2687.03	400.00[a]
Salar de Olaroz-Cauhcari	984.03	3900.00	318.81	842.45	5698.60	136.00	4875.93	1393.62	937.00
Salar de Rincon	470.45	3722.00	203.18	779.35	2811.20	199.00	2394.96	1171.16	287.00
Salar de Incaguasi	191.63	3470.00	165.43	762.05	1045.30	92.00	680.53	701.31	95.00
Salar de Pocitos	465.66	3665.00	213.93	825.09	2543.60	108.00	2326.39	501.13	60.00
Salar Grande	520.47	3410.00	256.31	843.71	8772.10	107.00	6712.67	1621.90	332.00
Salar de Arizaro	2133.53	3470.00	110.78	850.94	6736.90	147.00	5879.00	1927.77	188.00
Salar de Rio Grande	163.41	3665.00	150.51	722.05	1380.70	247.00	656.29	964.86	398.00
Salar de Liullaillaco	130.48	3755.00	178.98	692.39	1233.60	200.00a	484.86	1033.09	316.00
Laguna de Guayatayoc	564.16	3400.00	457.82	814.39	8772.10	72.00	6712.67	1621.90	96.00
Laguna de los Pozuelos	801.83	3660.00	580.03	789.90	3932.20	50.00[c]	1401.47	329.70	470.00[d]
Salar de Hombre Muerto	732.72	3967.00	219.76	805.75	3888.20	167.00	3974.44	2040.44	628.00
Bolivia									
Salar de Empexa	587.88	3744.00	328.17	710.37	2254.10	239.00	1906.41	1672.52	213.00
Lake Poopo	2296.95	3694.00	689.47	782.53	72,639.65	125.00	21,042.27	8290.99	200.00
Salar de Coipasa	4984.93	3665.00	488.51	815.90	72,639.65	145.00	21,042.27	8290.99	258.00
Salar de Uyuni	12,617.90	3660.00	337.02	831.61	47,350.80	123.00	34,257.21	22,949.54	715.00
Chile									
Salar de Atacama	3522.41	2304.00	96.74	1031.75	15,658.90	181.00	14,418.37	8040.31	1000.00
Salar de Coposa	141.90	3738.00	374.82	700.79	1126.30	20.00	1154.65	1024.09	16.00
Salar del Huasco	56.09	3785.00	397.92	724.67	1479.10	93.00	1408.39	1458.38	160.00
Salar de Ascotan	270.29	3724.00	357.22	701.73	1795.80	29.00	650.17	1534.80	47.00
Salar de Carcote	74.10	3693.00	369.83	706.26	490.80	234.00	223.96	366.76	217.00
Salar de Punta Negro	420.00	2950.00	78.38	902.52	4196.50	20.00	3986.10	1202.79	350.00
Salar de Aguilar	88.88	3320.00	152.37	663.09	560.80	113.00	367.22	559.20	367.00
Salar de la Isla	167.86	3960.00	140.87	649.50	751.10	62.00	353.60	590.49	402.00
Salar de las Parinas	41.82	3960.00	136.70	657.05	675.30	49.00	188.06	616.92	130.00
Salar de Pedernales	380.70	3351.00	144.03	721.58	11,048.70	221.00	3912.10	2335.51	520.00
Salar de Maricunga	213.70	3750.00	226.52	579.63	2420.60	36.00	1536.42	1834.95	319.00
Salar de Negro Fancisco	99.93	3750.00	269.08	514.99	699.30	149.00	568.09	599.95	408.00

[1] (GoogleEarthPro, 2022).
[2] (Farr et al., 2007).
[3] (Muñoz-Sabater et al., 2021).
[4] (Haran, 2015).
[5] (Lehner et al., 2008).
[6] (López Steinmetz and Salvi, 2021).
[7] (GlobCover., 2009).
[8] (Gómez et al., 2019).
[a] (mean values of adjacent salars).
[b] (Doran et al., 2010).
[c] (Murray et al., 2019).
[d] (GHD, 2019).

potential temperature; air density; Maximum sunshine duration and extra-terrestrial radiation; vapor pressure deficits; and average wind direction and speed. While evaplib.py calculates evaporation for different equations: Penman open water evaporation, Makkink, Priestley and Taylor, Penman Monteith, and Penman-Monteith (actual evapotranspiration); aerodynamic resistance from wind-speed and roughness parameters; sensible heat flux from temperature variations; and analytical rainfall interception model (Gash, 1979). Further details can be found in (GitHub - Kirubaharan/hydrology: Using Python for developing hydrological models and remote sensing workflow.)

4. Python scripts: Jupyter notebook using Python language developed by the author for data manipulation and analysis such as: merge raw data files, reading/writing of NetCDF files, simulate evaporation models, calculate windspeed resultant, etc.
5. Geographic information System (GIS): ArcGIS Desktop v10.7.1 developed by Environmental Systems Research Institute (ESRI) (2019) for spatial data manipulation and generation.

Previous studies (e.g. Risacher and Fritz (2009)) have attempted to relate lithium concentrations in brine to diagnostic parameters for the identification of possible correlations, but no clear trends or understanding have been identified. A recent example (López Steinmetz and Salvi, 2021), used mean Li concentration in brine vs salt pan area relationship which showed most salars clusters along mean Li axis (x-axis), with Coipasa, Atacama, and Uyuni as outliers (see Fig. 11(b) in López Steinmetz and Salvi (2021)). Indeed, most of the pan sizes of the salars are relatively small, and those that have the largest pan salt area in Andean Plateau, do not necessarily have the highest mean lithium concentration.

To help address the variation of parameters with respect to lithium

concentration, diagnostic factors of salars' regional correlations proposed as:

$$Li_f^s = \frac{Li^s}{dp^s} \quad (2)$$

where Li^s is the mean lithium concentration of salar (s), dp^s is the diagnostic parameter of describing the features of the salar (s) (see Table 2), and Li_f^s is normalised lithium factor. Table S.1 in Supplementary data illustrates Li_f^s values generated by Eq. (2). This factor represents the degree of diagnostic parameter's contribution in lithium evolution in relevant salar. In fact, it helps to identify which salars have in context or homogenous lithium proportion, and which is not (i.e., anomaly). For example (from Table S1 in supplementary data), Salars de Ascotan and Arizaro have similar Li/basin-area factors0.0026 and 0.0028, respectively, which imply that lithium concentration proportion to basin area is in context in both salars. In other words, both could have a similar lithium evolution environment with respect to basin area, while Salar de Aguilar whilst in a similar setting has a very different Li/basin-area factor of 0.654.

2.2.2. Identifying correlations between parameters

Accordingly, diagnostic factors have been used to develop a greater understanding of the lithium evolution environment context/pattern in Andean Plateau. The steps in the process are as follows:

1- Parameter manipulation: Plotting lithium against the related parameters overlaid by relevant diagnostic factors, to compare concepts.
2- Correlations: Plotting diagnostic factors, to investigate possible correlations.
3- Classification: Classify correlations, e.g., regional/local.
4- Clusters identification: Identify cluster groups and outliers.
5- Clusters validation: Multivariable analysis to validate group clusters.
6- lithium evolution environment: Identify salars' similarities/anomalies.

2.2.3. Multivariable analysis

Hierarchical clustering was used to identify dissimilarities (similarities) of variables based on different metrics such as Euclidean distance, Squared Euclidean distance, Manhattan (or city block) distance, Maximum distance (or Chebyshev distance), Mahalanobis distance, which may influence the shape of the clusters, as some elements may be relatively closer to one another under one metric than another. Additionally, linkage criterion which specifies the dissimilarity of sets as a function of the pairwise distances of observations in the sets, should also be set such as Maximum or complete-linkage clustering (Furthest), Minimum or single-linkage clustering (Nearest), Weighted average linkage clustering (or WPGMA), Centroid linkage clustering, or UPGMC, Ward, etc. More details can be found in (Nielsen, 2016).

Here, we used the standard Euclidean distance metric, and four commonly linkage criterions to explore pairwise distances sensitivity as follow, however researchers may adopt other methods for extra exploration:

- Nearest: the distance between two clusters is taken to be the distance between their closest neighbouring objects.
- Furthest: the distance between two clusters is the maximum distance between two objects in different clusters.
- Average: the distance between two clusters is calculated as the average distance between all pairs of objects in the different clusters.
- Ward: For each cluster, the means for all variables are calculated. Then, for each case, the squared Euclidean distance to the cluster means is calculated. These distances are summed for all of the cases. The cluster to be merged is the one which will increase the sum the least. That is, this method minimizes the increase in the overall sum of the squared within-cluster distances. This method tends to create clusters of small size.

Details of relevant formulation are beyond the scope of current research, and can be found in the wider literature, e.g. Szekely and Rizzo (2005).

3. Results and discussion

3.1. Parameters manipulation

Plotting lithium concentration [mg/l] against the diagnostic parameters enables relationships, where they exist, to be identified. Scatter plots of lithium concentration vs the parameters outlined in Table 1 are presented in Fig. 3 and show:

(a) Ground elevation - Generally high but shows three groups of salars at different levels 3400, 3750 and 4000 m.a.s.l. There is a limited single correlation against lithium concentration, with possible multilinear discrete relationships. Clearly, Atacama is an outlier with the lowest elevation and the highest lithium concentration. Thus, it is not possible to identify clear regional patterns of lithium distribution, or more precisely, limited parameter significance.
(b) Precipitation – possibility of an inverse relationship (Li proportional 1/p), as salars with high lithium concentration are located in a low precipitation zone, such as Atacama, Olaroz-Cauchari, and Uyuni. As for ground elevation, limited core correlation exists, with possible some discrete linear radial relationships from origin. Here, Atacama, Olaroz-Cauchari, Uyuni, Laguna de los Pozuelos, and Lake Poopo appears as outliers, away from the origin. Again, limited parameter significance is observed.
(c) Evaporation – seemingly a more random distribution, but with grouping around 275 mg/l and 1100 mm/annum. Again, limited core correlation with possibility of different linear relationships. Atacama, Olaroz-Cauchari, Laguna Blanca, and Negro Francisco appear to be outliers with limited parameter significance, again.
(d) TDS – random distribution with possible various linear radial relationships "spokes" radiating from origin. Like previous relationships, limited core correlation and parameters significance, with Atacama Olaroz-Cauchari as apparent outliers.
(e) Salt pan area – linear relationship for smaller areas can be observed, but with three significant outliers: Uyuni, Atacama and Coipasa, and with Lake Poopo and Salar de Arizaro just away from core correlation trend. Here, core correlation and parameter significance are evident. Hence, given pan size is relatively constant during salar lifetime then trend in Li concentration could indicate age of salar/development.
(f) Basin size – very similar to pan area but more scatter and Lake Poopo added to outliers as the largest basin size they have (share with Salar de Coipasa).
(g) Land cover – very similar to basin size (f)
(h) Volcanic – very similar again to (f) and (g)
(i) Salt pan area (detail) – generally speaking shows linear relationship between pan area and Li concentration.
(j) Basin area (detail) – a number of potential linear relationships can be identified.
(k) Land cover (detail) – like basin area (j)
(l) Volcanic (detail) – like (j) and (k)

In summary, it is not possible to relate lithium concentration to a significant number of the parameters describing the variation of the properties of the salars. In particular ground elevation, precipitation, evaporation, and TDS, cannot be related. It is, however, possible to relate lithium concentration to the area of the saltpan, basin, bare land cover, and volcanic formation. However, in general large salars are

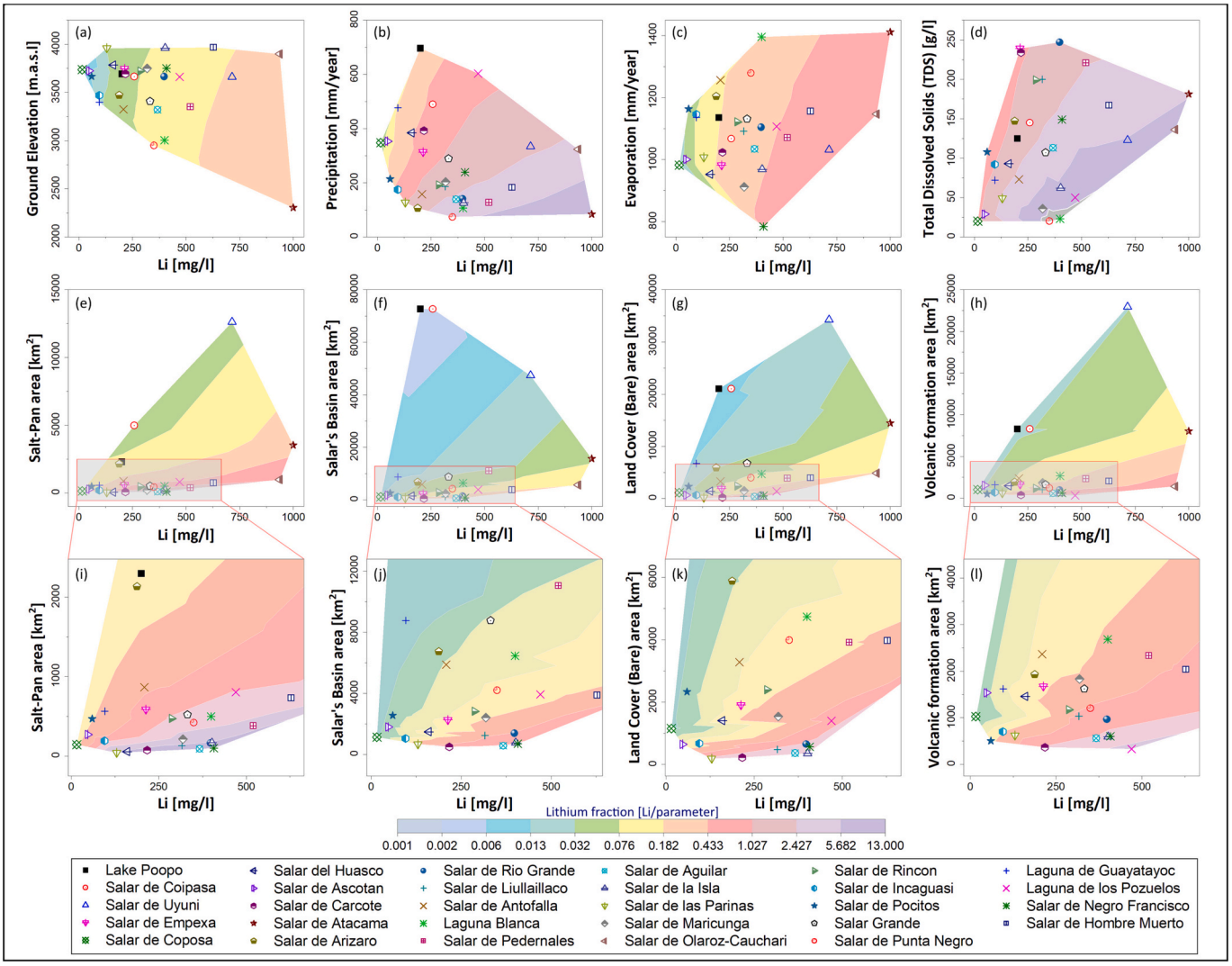

Fig. 3. Lithium verses selected parameters scatter plots. (a) to (h) plots between lithium concentration in salars' lake/pan [mg/l] verses pan/lake ground elevation [m.a.s.l], mean annual precipitation [mm/annum], mean annual evaporation [mm/annum], Total Dissolved Solids (TDS) [g/l], Salt-pan area [km^2], Salar's Basin area [km^2], basin's Bare area [km^2], and Basin's Volcanic rock area [km^2]. (i) to (l) are cluster zoom plots of (e) to (h), respectively. Plots from (a) to (d) shows correlations due to cloudy distribution, while (e) to (h) shows most of salars clusters close to bottom right corner, and some are away such as Lake Poopo, Uyuni, Coispasa, Atacama, and Olaroz-Cauchari Salars, as they have larger basins' area. Colour contour overlay maps represent relevant diagnostic fraction (Li/relevant basin's parameters. Here, salars within same colour zone are in context in lithium environment evolution, and those within higher values zones are outliers, as shows in zoom plots (i) to (l), such as Aguilar, Carcote, Negro Francisco, and la Isla Salars.

outliers such as Atacama, Uyuni, Poopo, and Coipasa. As for López Steinmetz and Salvi (2021) these results are unable to provide clear systematic outcomes about lithium concentration spatial variations/patterns, or about salars' similarities and/anomalies.

Revisiting Fig. 3 to examine these relationships using relevant overlaid diagnostic factor values (colour contour patterns), that indicate context/harmony degree of salars' lithium evolution environment (performance direction [logarithmic scale] from light cyan (high) to purple (low)):

(a) Ground elevation – Generally four zones (patterns) in range of 0.006–0.433 observed, most salars clustered in zones blue, green, and yellow, and only three (Atacama, Olaroz-Cauchari, and Uyuni) at the end (light brown) as outliers.
(b) Precipitation – Generally six patterns ranged 0.032–13.0 in context with precipitation patterns in Fig. 1(c), with Atacama as an outlier.
(c) Evaporation – Five patterns ranged 0.013–1.027 follow evaporation patterns (Fig. 1(d)), with Atacama, Olaroz-Cauchari, Uyuni, Negro Francisco, Hombre Muerto, and Pedernales as outliers.
(d) TDS – Five patterns ranged 0.433- > 13.0 with Laguna Blanca and Salar de Punta Negro as outliers.
(e) & (i) Salt pan area – Four main and three bottom limited patterns ranged 0.032–13.07. Here, Uyuni, Atacama, Coipasa, Lake Poopo, and Arizaro are NOT outliers as they are in context environment with others, and Salar del Huasco, Carcote, Aguilar, and Negro Francisco appear as outliers.
(f) & (j) Basin size – Five main and two bottom limited patterns ranged 0.002–1.027, with Salar de Carcote, Aguilar, la Isla, and Negro Francisco as outliers.
(g) & (k) Land cover – Four main and three bottom limited patterns ranged 0.006–2.427, with Liullaillaco and Rio Grande join the outliers as in (f).
(h) & (l) Volcanic – Similar patterns numbers as in (g) ranged 0.013–5.682, with Laguna de los Pozuelos join outliers as in (f)

In summary, individual diagnostic factors can be used to identify

relevant lithium evolution environment regional context, anomalies, and patterns in a systematic way, hence correlations across factors should be explored to examine potential relationships to improve system understanding.

3.2. Correlations and classifications

Given that limited correlation is identified by plotting diagnostic parameters against lithium concentration, the use of diagnostic factors (lithium/parameter) correlated against each other provided a more promising approach, as in Fig. 4(a), where (r) [Pearson's coefficient] > 0.5, 0.3 < r ≤ 0.5, and r < 0.3 refers to high, moderate, and low correlations, respectively. From 28 possible correlations, thirteen significant correlations are identified, as Eight ∈ high and Five ∈ moderate. Groups of Three and Five high correlations identified (r > 0.5) of: Elevation (Li_{Elev}), Evaporation (Li_{ET}), and Precipitation (Li_{Pr}); and Pan-salt area ($Li_{P\text{-}area}$), Bare land cover (Li_{LC}), Basin area ($Li_{B\text{-}area}$), and Volcanic rocks area (Li_{Geo}), respectively. Moderate correlations (r∈ (0.3,0.5]) of: TDS (Li_{TDS}) with Elevation, Precipitation, and Evaporation; and Volcanic rock with Pan-area and Evaporation recognized, while low correlations for other 15 relationships as r < 0.3. Noticeably, basin characteristics have limited correlation with weather and topographic patterns, indeed watershed and salt-pan sizes; land cover; and geological formation are not related to elevation, precipitation, and evaporation, apart from a moderate correlation of geology with evaporation (as factors), as regional patterns may partially be in context. TDS (salinity) is not a matter of basin characteristics, and only marginally of weather and topography, as recognized by the limited and moderate correlations (Fig. 4(a)), which is in context with López Steinmetz et al. (2018) findings TDS is a measure of the total ionic content of the brines. Whilst brine evolution in itself is necessary for lithium-rich salars, the concentration of lithium will depend on the source rocks providing specific

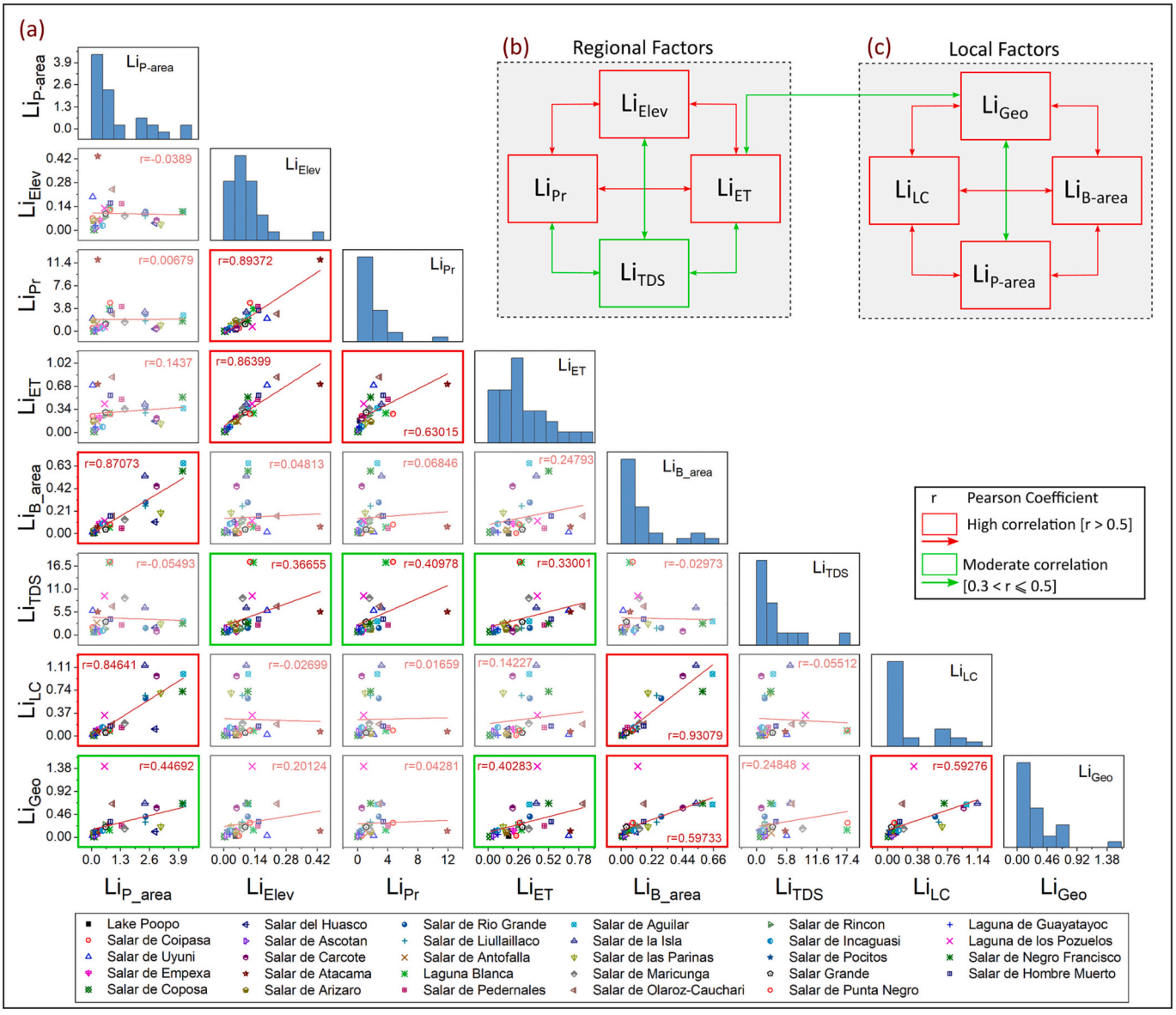

Fig. 4. (a) Scatter matrix plot of lithium-fraction illustrates 28 possible relevant correlations based on Pearson coefficient (r). Eight high positive correlation observed (highlighted in red) with r > 0.5, and Five positive moderate correlation (highlighted in green) with r∈(0.3,0.5]. Others (faded) have week positive and negative correlations. (b) and (c) lithium-fraction factors classifications based on correlation's degrees, high and moderate, respectively. Based on High correlation relationship (red arrows) (a), Regional Parameters assigned to parameters of lithium-elevation, −precipitation, and -evaporation linked to regional spatial patterns, and Local Parameters to lithium-pan area, −basin area, −land cover, and -geological formation (here, Volcanic rock) link to local basin characteristics. Moderate relationship (green arrows) follows same concept expect for lithium-geology parameter which linked to both groups.

lithium input. It is likely that watersheds/basins exist in which significant solutes can be leached to produce high TDS, but that they may be lacking in source rocks providing significant lithium mass.

Two such relationships emerge out of this process: regional and local (Fig. 4b and Fig. 4c). Regional covers factors such as elevation, precipitation and evaporation; local includes size of watershed, salar nucleus, land cover and geological outcrop in the watershed.

In general, the histogram of parametric distribution is skewed to the right, i.e., clustering around low values then sharply reduced towards higher values, with some gaps noticed which possibly due to dataset outliers, as in Li_{Pr}, Li_{Elev}, Li_{TDS}, and Li_{Geo}, or data splitting as in Li_{LC} and $Li_{B\text{-}area}$.

Fig. 4(a) exposed two groups of factors, Regional and Local, as in Fig. 4(b) and (c), respectively. Elevation (Li_{Elev}), Precipitation (Li_{Pr}), and Evaporation (Li_{ET}) are grouped under Regional Factors that are relevant to regional spatial patterns, building on Fig. 2(a), (b), and (c), respectively, pointing to similarities in lithium evolution environment at a regional scale. On the other hand, Local factors grouped basin's characteristics of Pan-salt area ($Li_{P\text{-}area}$), Basin area ($Li_{B\text{-}area}$), Geology (Li_{Geo}), and Land Cover area (Li_{LC}), as in Fig. 2(a), (c), and (d) respectively, expressing similarities in lithium evolution environment at a local scale, that may fully or partially participate or effect lithium concentration evolution. Fig. 5 shows details of the two groups, Local and Regional, and the following noticed:

(a) Pan area vs Basin area – majority low values expressing environments' context with three identified clusters A, B and C, where C are those salars with small pan/basin areas but high lithium concentration: Aguilar, Negro Francisco, la Isla, and Carcote with 367, 408, 402, and 217 mg/l of lithium, and 88.88, 99.93, 167.86, and 74.1 km^2 of Pan-salt area, respectively. Less variation in cluster B, where: Rio Grande, las Parinas, Liullaillaco, and Huasco having (Li/Pan area): 398/163.41, 130/41.82, 316/130.48, 160/56 [mg/km^2], respectively. In fact, salars in cluster A are more homogenous/in context than B and C, in lithium concentration proportion regarding plotted parameters. This concept is application for all plots in Fig. 5.

(b) Pan area vs Land cover – again majority of low values with two main cluster A and B, alike to (b) small bare area with high Li concentration in cluster B, where: Aguilar, Negro Francisco, Carcote, Rio Grande, las Parinas, and Liullaillaco having 367, 408, 217, 398, 130, and 316 mg/l, and two outliers: la Isla (402 mg/l), and Huasco (160 mg/l), respectively.

(c) Basin area vs Land cover – very similar to (a) having three clusters A, B and C, just Salar de Huasco joins A cluster, not B.

(d) Basin area vs Geology – very similar to (b) with two clusters A and B, just Rio Grande and Liullaillaco joins A, with Olaroz-Cauchari and los Pozuelos as outliers.

(e) Land cover vs Geology – as in (c) with three clusters A, B and C, just Negro Francisco moved to B, with Olaroz-Cauchari and los Pozuelos as outliers.

(f) Elevation vs Precipitation – majority lower values with Atacama as an outlier.

(g) Elevation vs Evaporation –like (f) but with greater spread again Atacama as an outlier which skews liner relationship.

(h) Precipitation vs Evaporation - like (g) but with greater spread again Atacama as an outlier which skews liner relationship.

(i) Elevation vs Precipitation –removing Atacama allows greater detail to be identified with four clusters A, B, C, and D. Punta Negro, Laguna Blanca, Pedernales, Hombre Muerto, Olaroz-

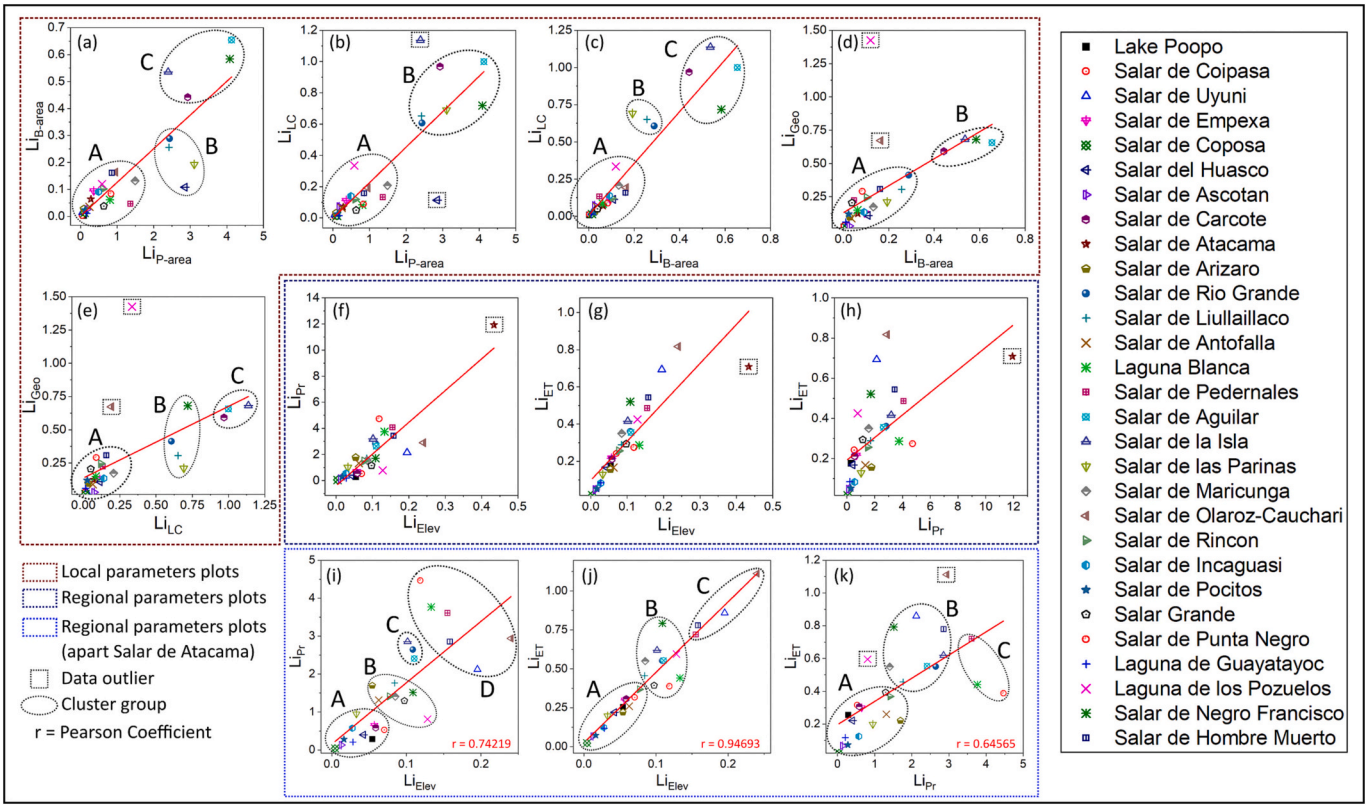

Fig. 5. Lithium-fraction parameters with Pearson's correlation factor (r) >0.5. (a) to (e) scatter plots of Local Parameters with recognized cluster groups (dotted ellipse) and outliers (dotted polygon). In plot (b) [$Li_{P\text{-}area}$ vs Li_{LC}] Salars to la Isla and de Huasco identified as outliers, while in (d) [$Li_{B\text{-}area}$ vs Li_{Geo}] and (e) [Li_{LC} vs Li_{Geo}] are Laguna de los Pozuelos and Salar de Olaroz-Cauchari, respectively. (f), (g), (h) are for Regional Parameters with only outlier recognized, Salar de Atacama, as clustering not clear, hence (i), (j), and (k) generate by excluding Salar de Atacama to differentiate possible cluster groups. In (k) [Li_{Pr} vs Li_{ET}] Laguna de los Pozuelos and Salar de Olaroz-Cauchari also recognized as outliers, which may refer to possible basin's environment similarity.

Cauchari, and Uyuni covered in D, having higher lithium proportion to ground level, as (Li/level): 350/2950, 400/3005, 520/3351, 628/3967, 937/3900, and 715/3660, respectively. While la Isla, Rio Grande, and Aguilar yielded in C, and other in B and A.

(j) Elevation vs Evaporation - removing Atacama allows greater detail to be identified with three clusters A, B, and C. Here, Olaroz-Cauchari, Uyuni, Hombre Muerto, and Pedernales covered in C, others in B and A proving very high correlations ($r = 0.94$), expressing strong harmony of patterns within clusters, then their lithium environment evolution.

(k) Precipitation vs Evaporation - removing Atacama allows greater detail to be identified as in (j), just C covered only Hombre Muerto, Laguna Blanca, and Coipasa and with Olaroz-Cauchari and Los Pozuelos as outliers.

Map projections of clusters in Fig. 5 illustrated in Fig. S4 in supplementary data.

3.3. Cluster validation

Multivariable sensitivity analysis of Regional Factors shows Salar de Atacama has its own, major cluster using Nearest, Furthest, and Average linkage, and a separate sub-cluster in Ward, as shown in Fig. S2 in Supplementary data. Although many salars are in line with regional patterns of annual precipitation and evaporation like Salar de Atacama, as in Fig. 2c and d respectively, however Atacama has the lowest elevation than others leading to its being considered as its own major cluster. At a regional scale, Atacama has a different lithium-environment than others, which evident by the fact it has the highest lithium concentration that is matching the finding of apparent clusters. In the case of Atacama, then much research has been undertaken to close the basin water balance, e.g. (Boutt et al., 2021; Marazuela et al., 2018; Moran et al., 2022). Whereas Marazuela et al. (2018) assume recharge within hydrological basin's regime, Moran et al. (2022) concludes that basin recharge may extend beyond hydrological watershed, e.g., from other adjacent basins and is unlikely to be derived from contemporary rainfall. Both conclusions, even though they are conflicting, may be applicable on Atacama, but may not on others, as current results show. In other words, any scientific conclusions built on Salar de Atacama may be at best partially applicable to other salars in the region.

Local Factors shows some membership changes over different adopted linkage methods. For example, cluster No.1 in Nearest linkage covers 20 salars (from total of 29 salars), but this is not the case in other linkage cases as cluster which cover 12, 11, and 12 salars for Furthest, Average, and Ward, respectively, as shown in Fig. S3 in Supplementary Data, in which Salar de Incagausi moved from cluster No.1 to No.2 in Average linkage, and then returns back to No.1 in Ward. On the other hand, sensitivity analysis identifies Laguna de los Pozuelos as outlier, as has single sub-cluster over adopted linkage methods. The same behaviour noticed with Salar de Negro Francisco and Salar de Aguilar. Noticeably, large salars coincide in one cluster (No.1), however some small salars located within the same cluster which may be due to their maturity in terms of lithium evolution. Laguna de los Pozuelos found as outlier in both methods, others (i.e., Olaroz-Cauchari, la Isla, Huasco, Negro Francisco, and Aguilar) possibly being in grey area or cliff edge of cluster zones.

3.4. Lithium evolution environment

To understand the spatial distribution of the parametric relationships, lithium concentration, regional and local lithium factors are plotted (Fig. 6) and their values contoured.

Examining Fig. 6a shows that there is a general regional pattern of higher values in the central area (~1000 mg/l) with lower values in the central southern part of the region (60–130 mg/l). There are definite "Hotpots" to the north of the region: Salar de Uyuni (SdU) and Caoipasa in the central area: Atacama and Cauchari-Oleroz, and in the south-east – Hombre Muerto. What is clear is that elevated concentrations of lithium exist outside of 66°30′ to 68 ° 30' /30 ° – 24 ° proposed by López Steinmetz and Salvi (2021).

Regional: The general regional patterns (Fig. 6b) are much harder to discern than for the lithium concentration itself as the distribution is heavily dominated by the Salar de Atacama (SdA) (13.1), most of the remaining values are 2 or less. However, there are exceptions such as at Salar de Punta Negra 5.12, Pedernales 4.71, Hombre Muerto 4.17, and Uynui 3.95. SdA presents such a dominant value due to its relatively low elevation (2500 m ASL), low rainfall and high evaporation. These group of salars could show the importance of flow through – higher rainfall and greater evaporation leading to greater lithium mass brought into the salar and, ultimately, via evaporative processes concentration of lithium. This is predicated on the basis that inflow waters contain high enough concentrations of lithium for long periods of time.

Local: Examining Fig. 6c shows that as for the distribution of regional parameters, the general local patterns are much harder to discern than for the lithium concentration itself. There are hots spots in the south-west part of the area as well as the north-west. These consist of the smaller salars such as in the east of the area: Los Puozuelos (2.47), Carcote/Ascotan (4.93), and in the south-west: Aguila (6.46) Francesco Negra (6.06). These are smaller salars in close proximity to source rocks, i.e., volcanic. This contradicts the assumption that only larger salars have higher lithium concentrations as postulated by López Steinmetz and Salvi (2021).

3.5. Potential lithium sources

Siliciclastic sedimentary rock (Fig. 7 - Geological map - pink colour) such as Carbonate and Evaporitic may well have a role in lithium evolution, in particular by providing a leachable source of lithium. There is a potential to have a greater propensity for dissolution by either surface or groundwaters and could be re-worked after the lithium is concentrated in these deposits. To investigate this phenomenon, the outcrop of these geologies are included with Volcanic rocks to determine whether they improve the correlation with lithium factors. The majority of the outcrop of these geological units covers the northern, central-eastern and western parts for the area. The relationships between the factors and normalised lithium concentration were re-calculated, as in Fig. 7 - Scatter plots, and a noticeable improvement in the correlation. Geology correlations are modified as follows: Pan area improved about twice, $r = 0.44$ to 0.76, boost correlation to "high" zone; Evaporation slightly improved, $r = 0.40$ to 0.41, but outliers exposed clearly (compare with Fig. 4(a)); correlation for basin area significantly improved from $r = 0.59$ to 0.9; and the relationship with Land Cover increased from $r = 0.59$ to 0.8, as in Fig. 7(a), (b), (c), and (d), respectively. The outliers were as follow:

(a) Salar de la Isla, Aguilar, and Negro Francisco;
(b) Salar de la Isla, Aguilar, Negro Francisco, Atacama, and Uyuni;
(c) Salar de Carcote; and
(d) Non – but possibly Carcote and Negro Francisco.

The lithium environment for Salar de los Pozuelos is modified and improved in relation to those identified in cluster A, comparing with Fig. 4(a). However, the correlation for Aguilar, Negro Francisco, and Carcote is noticeably reduced in all cases in Fig. 7 having small size and high lithium concentration. This means that more investigation is required to identify relevant lithium sources since no extra sources has been added by this process. For the case of Salar de Olaroz-Cauchari, which in common with Atacama and Uyuni in having high lithium concentration and evaporation rate, only the last two stands out in Fig. 7 (b), as they have larger sizes and extra potential lithium sources.

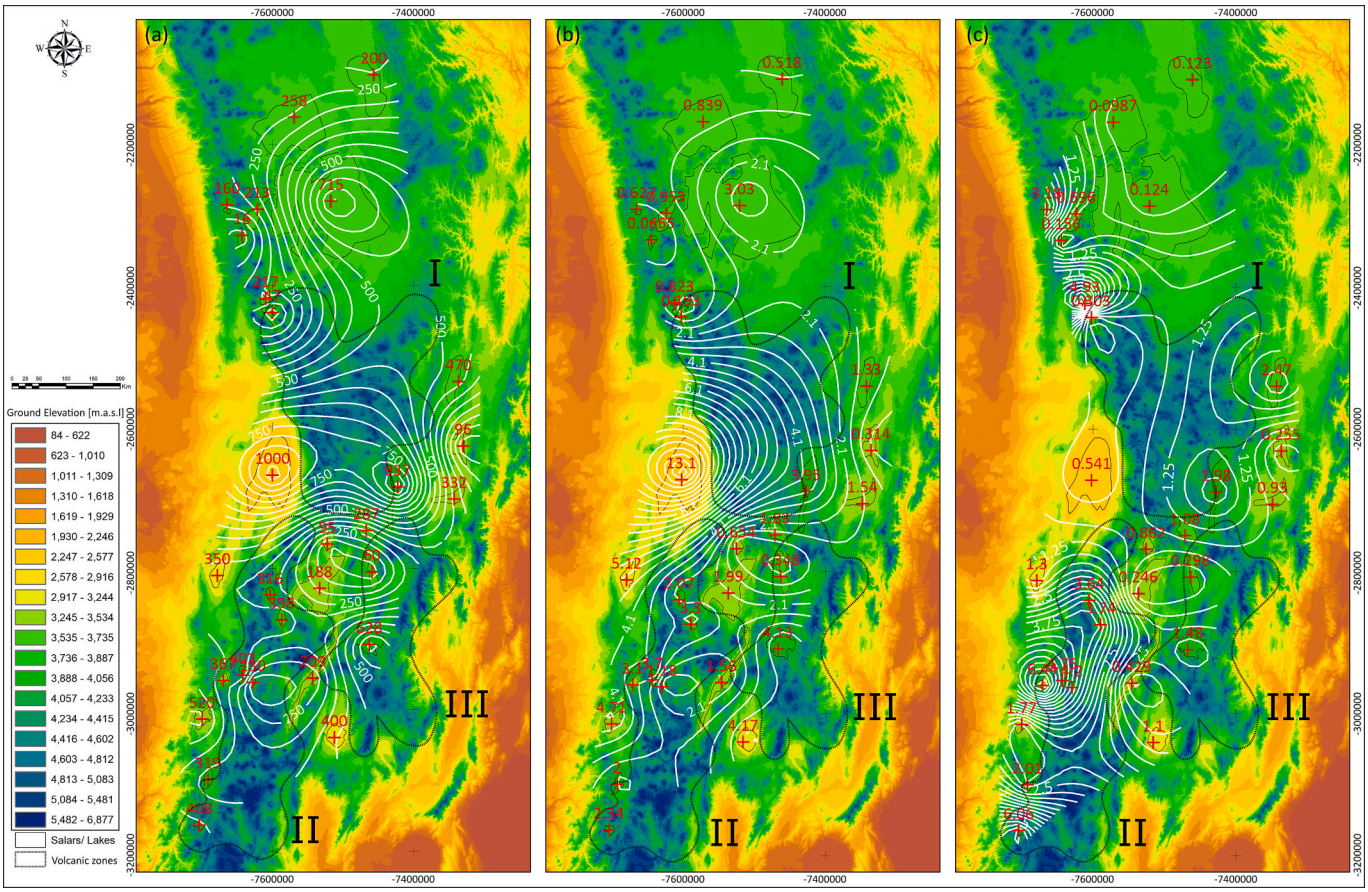

Fig. 6. Contour maps of source and lithium Factors in High Andes. 6(a) illustrated the distribution of lithium concentration across the area. 6(b) illustrates the distribution of lithium regional factors and 6(c) the spatial distribution of lithium local factors. The black dotted line represents the areas with high density of volcanoes as represented by the density of peaks.

3.6. Implications for development of lithium operations from salars

The work presented here has demonstrated that whilst there are similarities between the parameters characterising salars, there are still significant differences. Importantly Salar de Atacama is identified as an end member and given the amount of work invested and published then it is important to recognise how it relates to other salars and to put it into context. The corollary of the differences between salars is that there is no single source of best practice and, therefore, no unified set of rules that can work for all the salars. To dela with this situation, a flexibility of approach is required that informs the operator what to do and how to approach the problem, and not just rely on a single indicators, e.g. AWARE (Boulay et al., 2017). Further, any assessment of environmental impact needs to take into account the similarities and differences as identified by this paper and that detailed studies developing system understanding and subsequent modelling is required to deal with this variability in terms of different scales: spatial - project, salar, basin and time – seasonal, decades and millennia. This complexity and the need to consider the complexity of the systems has implications for the current Life Cycle Assessment approaches and needs further study. Further, different tools are required that are more fully featured than project based Environmental Impacts Assessments. Examples of this include Strategic Environmental and Social Assessments, which operate at a larger spatial scale such as basin, country or regional (Petavratzi et al., 2022b). This is also reflected in the need to change from monitoring operations to monitoring systems. Further, resources and reserve estimation methodologies need to account for the variability of salars identified in this work.

4. Conclusions

This work has used a range of parameters to understand the relationship between different salars within the lithium triangle countries (Argentina, Bolivia and Chile): lithium concentration, elevation, precipitation, evaporation, land cover, geology, pan size and basin size. Normalisation using lithium concentration is required to identify a relationship and subsequent correlation between the different parameters – ratio of Li concentration to the parameter under investigation. Two such relationships emerge out of this process: regional and local. Regional covers factors such as elevation, precipitation and evaporation; local includes size of watershed, salar nucleus, land cover and geological outcrop in the watershed.

Regional – climate influence is loosely related to elevation (orographic effect), but importantly north-south air masses produce higher rainfall and lower evaporation at higher elevations. The lowest salar, Atacama is the most western and so impacted by the Atacama Desert climate. This means that whilst evaporation is highly correlated to elevation, rainfall isn't linked as well. So salar location is not a good predictor of climate and a greater understanding of weather patterns is required to relate lithium concentration to current climate. However, this relates to the contemporary situation and it is known that the past climate has been significantly wetter, particularly related to both surface water input (e.g. lake levels in the Salar de Uyuni) and groundwater recharge (e.g. Salar de Atacama).

Local – very significant cluster around smaller salars, but with a spread of the ratio of lithium to size parameters. The majority of the salars studied have a similar size (watershed size for the majority <5000 km^2). This leads to clustering around the parameter with increasing

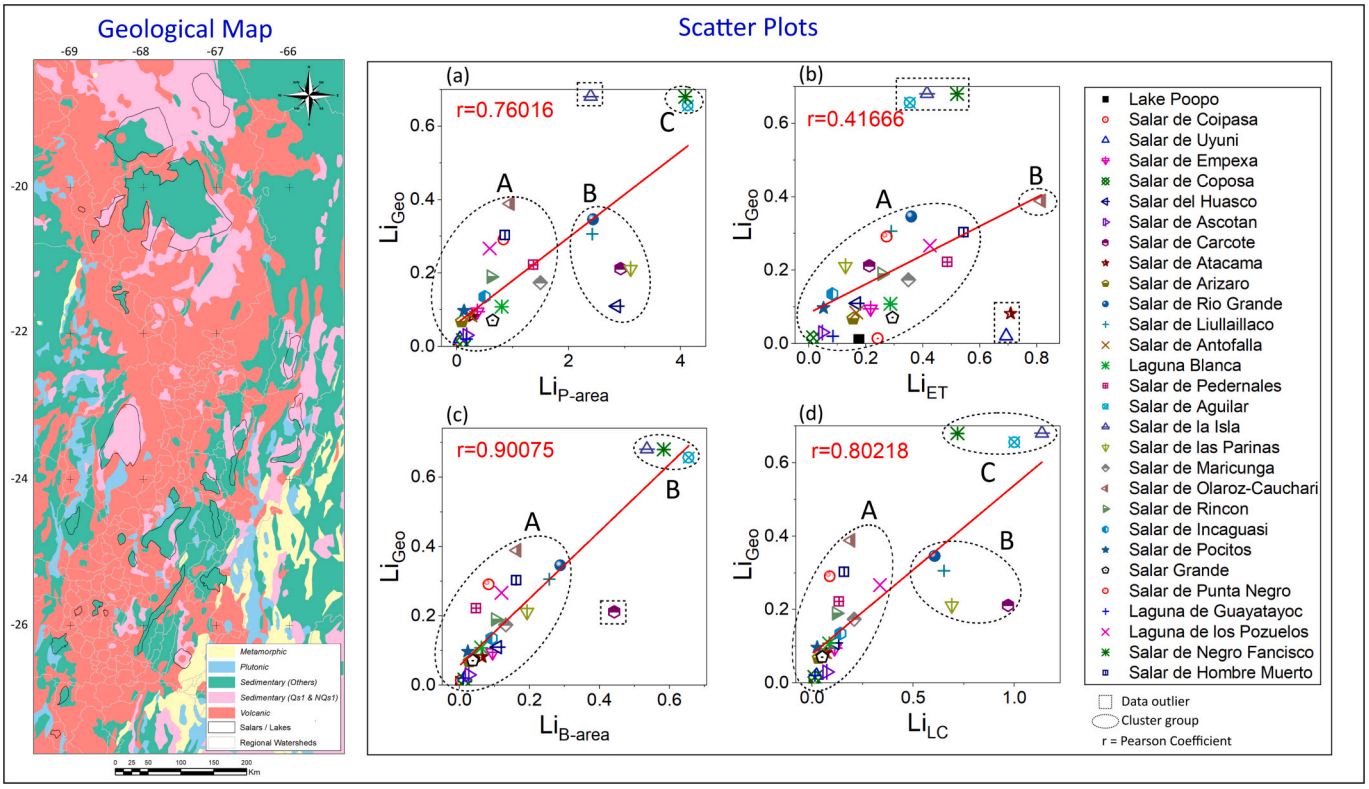

Fig. 7. Illustrates regional geological map classified by rock types and scatter plots with other parameters with high correlations relationships (r > 0.5). The geological map is as in Fig. 2(c), except sedimentary rock type Siliciclastic [light pink] apart of other types, such as Carbonate and Evaporitic which possibly participate in lithium evolution. Scatter plots of lithium-geology fraction parameter vs other parameters generated, but only High and Moderate correlations relationship shown, as others have low correlations, and cluster groups and outliers recognized. Pearson coefficient (r) improved in (a) from about 0.44 to 0.76, (b) 0.4 to 0.41, (c) 0.59 to 0.9, and (d) 0.59 to 0.80. In plots (c) and (d), Laguna de los Pozuelos and Salar de Olaroz-Cauchari not outliers, as in Fig. 5(d) and (e).

lithium concentration. Given the timescales required to accumulate lithium in any salar, this clustering could be related to developmental path and the age of the salar.

Salar de Atacama is an end member particularly in relation to elevation and climatic parameters. However, it does have features that are common to most other salars. One important example is the lagunas on which the Flamingos are dependent on for food and breeding sites. Salar de Uyuni, due to its size and lithium elevated concentration, is also an exception. However, similarly to Atacama, Salar de Uyuni has other unique features such as elevated magnesium concentrations and its higher seasonal rainfall resulting in annual flooding. The former results in problems in terms of processing the brines and the latter means that annual flooding of the salar surface occurs resulting in surface ponding in contrast to Atacama and other salars where the lagunas are groundwater fed.

Lithium availability from source rocks and time to accumulate lithium in the salars is key to developing an economic exploitable lithium resource. Whilst the larger salars have significant lithium mass, smaller salars show greater lithium concentration that belies their size. This could be due to the proximity of lithium sources to these salars related to volcanoes and their role in bringing lithium to the surface, which affects exploration as it can identify smaller salars that have hotspots of lithium that could provide economic amounts for extraction.

This work has provided a framework by which salars can be placed in context of both their past and current state of development. Further work could examine the impact of volcanic "clusters" related to lithium concentration/time basis of its evolution; understand the reason for smaller salars to have elevated lithium concentration; use this approach for other parameters including resources and reserves. In particular, the 3D variation of lithium source rocks needs to be established both in terms of what rocks could have been the source of lithium and how leachable they are. By understanding the spatial distribution of source rocks (e.g. volcanically derived Ignimbrites) over the catchments supplying the salars the genesis of the lithium rich brines can be established. Finally, this work illustrates the complexities of salar systems and that any policy interventions need to take this variation into account.

CRediT authorship contribution statement

Jafar Al-Jawad: Writing – original draft, Conceptualization, Methodology, Validation, Formal analysis.

Andrew Hughes: Writing – review & editing, Supervision, Resources, Validation,

Evi Petavratzi: discussion of ideas and editing final draft.

John Ford: discussion of ideas and editing final draft.

Declaration of competing interest

The authors declare that they have no known competing financial interests or personal relationships that could have appeared to influence the work reported in this paper.

Data availability

Data will be made available on request.

Acknowledgements

Authors publish with the permission of the Executive Director of the British Geological Survey (UKRI/NERC). Kathryn Goodenough is thanked for her contributions as BGS internal reviewer. This work is supported by the UK's Natural Environment Research Council funded

Lithium for Future Technology project (NE/V006932/1). Scott Hynek, USGS, is acknowledged for his useful and insightful discussion related to this paper.

Appendix A. Supplementary data

Supplementary data to this article can be found online at https://doi.org/10.1016/j.scitotenv.2023.167647.

References

Allen, R.G., Pereira, L.S., Raes, D., Smith, M., 1998. Crop Evapotranspiration. Guidelines for Computing Crop Water Requirements.

Boulay, A.-M., Bare, J., Benini, L., Berger, M., Lathuillière, M.J., Manzardo, A., Margni, M., Motoshita, M., Núñez, M., Pastor, A.V., Ridoutt, B., Oki, T., Worbe, S., Pfister, S., 2017. The WULCA consensus characterization model for water scarcity footprints: assessing impacts of water consumption based on available water remaining (AWARE). Int. J. Life Cycle Assess. 23 (2), 368–378. https://doi.org/10.1007/s11367-017-1333-8.

Boutt, D.F., Hynek, S.A., Munk, L.A., Corenthal, L.G., 2016. Rapid recharge of fresh water to the halite-hosted brine aquifer of Salar de Atacama, Chile. In: Hydrological Processes, vol. 30, pp. 4720–4740.

Boutt, D.F., Corenthal, L.G., Moran, B.J., Munk, L., Hynek, S.A., 2021. Imbalance in the modern hydrologic budget of topographic catchments along the western slope of the Andes (21–25°S): implications for groundwater recharge assessment. Hydrogeol. J. 29 (3), 985–1007. https://doi.org/10.1007/s10040-021-02309-z.

Bradley, D., Munk, L., Jochens, H., Hynek, S., Labay, K.A., 2013. A preliminary deposit model for lithium brines [Report](2013-1006). (Open-File Report, Issue. U. S. G. Survey). http://pubs.er.usgs.gov/publication/ofr20131006.

Brêda, J.P.L.F., de Paiva, R.C.D., Collischon, W., Bravo, J.M., Siqueira, V.A., Steinke, E. B., 2020. Climate change impacts on South American water balance from a continental-scale hydrological model driven by CMIP5 projections. Clim. Chang. 159 (4), 503–522. https://doi.org/10.1007/s10584-020-02667-9.

Corenthal, L.G., Boutt, D.F., Hynek, S.A., Munk, L.A., 2016. Regional groundwater flow and accumulation of a massive evaporite deposit at the margin of the Chilean Altiplano. Geophys. Res. Lett. 43, 8017–8025.

De Bruin, H.A.R., 1987. In: Hooghart, J.C. (Ed.), From Penman to Makkink.

Doran, P.T., Lyons, W.B., McKnight, D.M. (Eds.), 2010. Life in Antarctic Deserts and other Cold Dry Environments: Astrobiological Analogs. Cambridge University Press. https://doi.org/10.1017/CBO9780511712258.

Environmental Systems Research Institute (ESRI), 2019. ArcGIS Desktop 10.7.1. In (Version 10.7.1). www.esri.com.

Farr, T.G., Rosen, P.A., Caro, E., Crippen, R., Duren, R., Hensley, S., Kobrick, M., Paller, M., Rodriguez, E., Roth, L., Seal, D., Shaffer, S., Shimada, J., Umland, J., Werner, M., Oskin, M., Burbank, D., Alsdorf, D., 2007. The shuttle radar topography mission. Rev. Geophys. 45 (2) https://doi.org/10.1029/2005rg000183.

Gash, J.H.C., 1979. An analytical model of rainfall interception by forests. Q. J. R. Meteorol. Soc. 105 (443), 43–55. https://doi.org/10.1002/qj.49710544304.

GHD, 2019. Preliminary Economic Assessment (PEA) - Pozuelos -, Pastos Grandes Project, NI 43-101 Technical Report, Salta, Argentina.

GlobCover., 2009. Land Cover, Central and South America. ESA. https://databasin.org/datasets/693f573b98834d1cbcc364e7f0b8e5db/.

Gómez, J., Schobbenhaus, C., Montes, N.E., compilers, 2019. *Geological Map of South America 2019*. Scale 1:5 000 000. Commission for the Geological Map of the World (CGMW), Colombian Geological Survey, and Geological Survey of Brazil, Paris.

GoogleEarthPro, 2022. High Andes Salars' borders. In (Version 7.3) Google LLC. https://www.google.com/intl/en_uk/earth/about/versions/.

Hamman, E., Post, V., Kahfahl, C., Prommer, H., Simmons, C.T., 2015. Numerical investigation of coupled density-driven flow and hydrogeochemical processes below playas. Water Resour. Assoc. 51, 9338–9352.

Haran, K., 2015. Meteorology and Evaporation Function Modules for Python. https://github.com/Kirubaharan/hydrology.

Hargreaves, G.H., Samani, Z.A., 1985. Reference crop evapotranspiration from temperature. Appl. Eng. Agric. 1 (2), 96–99. https://doi.org/10.13031/2013.26773.

Houston, J., 2006a. Evaporation in the Atacama Desert: an empirical study of spatio-temporal variations and their causes. J. Hydrol. 330, 402–412. https://doi.org/10.1016/j.jhydrol.2006.03.036.

Houston, J., 2006b. Variability of precipitation in the Atacama Desert: its causes and hydrological impact. Int. J. Climatol. 26 (15), 2181–2198. https://doi.org/10.1002/joc.1359.

Houston, J., Hartley, A.J., 2003. The central Andean west-slope rainshadow and its potential contribution to the origin of hyper-aridity in the Atacama Desert. Int. J. Climatol. 23 (12), 1453–1464. https://doi.org/10.1002/joc.938.

Houston, J., Butcher, A., Ehren, P., Evans, K., Godfrey, L., 2011. The evaluation of brine prospects and the requirement for modifications to filing standards. Econ. Geol. 106 (7), 1225–1239.

IEA, 2021. The Role of Critical Minerals in Clean Energy Transitions.

Lehner, B., Verdin, K., Jarvis, A., 2008. New global hydrography derived from spaceborne elevation data Eos. Trans. Am. Geophys. Union 89 (10), 93–94. https://doi.org/10.1029/2008EO100001.

López Steinmetz, R.L., Salvi, S., 2021. Brine grades in Andean salars: when basin size matters a review of the Lithium triangle. Earth Sci. Rev. 217 https://doi.org/10.1016/j.earscirev.2021.103615.

López Steinmetz, R.L., Salvi, S., Gabriela García, M., Peralta Arnold, Y., Béziat, D., Franco, G., Constantini, O., Córdoba, F.E., Caffe, P.J., 2018. Northern Puna Plateau-scale survey of Li brine-type deposits in the Andes of NW Argentina. J. Geochem. Explor. 190, 26–38. https://doi.org/10.1016/j.gexplo.2018.02.013.

López Steinmetz, R.L., Salvi, S., Sarchi, C., Santamans, C., López Steinmetz, L.C., 2020. Lithium and brine geochemistry in the Salars of the southern Puna, Andean Plateau of Argentina. Econ. Geol. 115 (5), 1079–1096. https://doi.org/10.5382/econgeo.4754.

Marazuela, M.A., Vazquez-Sune, E., Custodio, E., Palma, T., Garcia-Gil, A., Ayora, C., 2018. 3D mapping, hydrodynamics and modelling of the freshwater-brine mixing zone in salt flats similar to the Salar de Atacama (Chile). J. Hydrol. 561, 223–235. https://doi.org/10.1016/j.jhydrol.2018.04.010.

Marazuela, M.A., Vazquez-Sune, E., Ayora, C., Garcia-Gil, A., 2020. Towards more sustainable brine extraction in salt flats: learning from the Salar de Atacama. Sci. Total Environ. 703, 135605 https://doi.org/10.1016/j.scitotenv.2019.135605.

Meixner, A., Alonso, R.N., Lucassen, F., Korte, L., Kasemann, S.A., 2021. Lithium and Sr isotopic composition of salar deposits in the Central Andes across space and time: the Salar de Pozuelos, Argentina. Mineral. Deposita 57 (2), 255–278. https://doi.org/10.1007/s00126-021-01062-3.

Moran, B.J., Boutt, D.F., McKnight, S.V., Jenckes, J., Munk, L.A., Corkran, D., Kirshen, A., 2022. Relic Groundwater and Mega Drought Confound Interpretations of Water Sustainability and Lithium Extraction in Arid Lands. https://doi.org/10.1002/essoar.10510758.1.

Munk, L., Hynek, S., Bradley, D.C., Boutt, D., Labay, K.A., Jochens, H., 2016. Lithium brines: a global perspective. In: Rare Earth and Critical Elements in Ore Deposits, 18, pp. 339–365. https://doi.org/10.5382/Rev.18.14.

Munk, L.A., Boutt, D.F., Hynek, S.A., Moran, B.J., 2018. Hydrogeochemical fluxes and processes contributing to the formation of lithium-enriched brines in a hyper-arid continental basin. Chem. Geol. 493, 37–57. https://doi.org/10.1016/j.chemgeo.2018.05.013.

Muñoz-Sabater, J., Dutra, E., Agustí-Panareda, A., Albergel, C., Arduini, G., Balsamo, G., Boussetta, S., Choulga, M., Harrigan, S., Hersbach, H., Martens, B., Miralles, D.G., Piles, M., Rodríguez-Fernández, N.J., Zsoter, E., Buontempo, C., Thépaut, J.-N., 2021. ERA5-Land: a state-of-the-art global reanalysis dataset for land applications. Earth Syst. Sci. Data 13 (9), 4349–4383. https://doi.org/10.5194/essd-13-4349-2021.

Murray, J., Nordstrom, D.K., Dold, B., Romero Orue, M., Kirschbaum, A., 2019. Origin and geochemistry of arsenic in surface and groundwaters of Los Pozuelos basin, Puna region, Central Andes, Argentina. Sci. Total. Environ. 697, 134085 https://doi.org/10.1016/j.scitotenv.2019.134085.

Nielsen, F., 2016. Hierarchical clustering. In: Nielsen, F. (Ed.), Introduction to HPC with MPI for Data Science. Springer International Publishing, pp. 195–211. https://doi.org/10.1007/978-3-319-21903-5_8.

Oyarzún, J., Oyarzún, R., 2011. Sustainable development threats, inter-sector conflicts and environmental policy requirements in the arid, mining rich, northern Chile territory. Sustain. Dev. 19 (4), 263–274. https://doi.org/10.1002/sd.441.

Penman, H.L., 1948. Natural evaporation from open water, Bare soil and grass. Proc. R. Soc. Lond. A Math. Phys. Sci. 193 (1032), 120–145. http://www.jstor.org/stable/98151.

Penman, H.L., 1956. Evaporation: an introductory survey. Neth. J. Agric. Sci. 4, 9–29.

Penman, H.L., 1963. Vegetation and hydrology. (Technical Communication No. 53, Commonwealth Bureau of Soils, Harpenden) Commonwealth Agricultural Bureaux, Farham Royal, 1963. Pp. v, 124: 72 Tables. 20s. Q. J. R. Meteorol. Soc. 89 (382), 565–566. https://doi.org/10.1002/qj.49708938220.

Petavratzi, E., Sanchez-Lopez, D., Hughes, A., Stacey, J., Ford, J., Butcher, A., 2022a. The impacts of environmental, social and governance (ESG) issues in achieving sustainable lithium supply in the Lithium Triangle. Miner. Econ. 35 (3), 673–699. https://doi.org/10.1007/s13563-022-00332-4.

Petavratzi, E., Sanchez-Lopez, D., Hughes, A., Stacey, J., Ford, J., Butcher, A., 2022b. The impacts of environmental, social and governance (ESG) issues in achieving sustainable lithium supply in the Lithium Triangle. Miner. Econ. https://doi.org/10.1007/s13563-022-00332-4.

Priestley, C.H.B., Taylor, R.J., 1972. On the assessment of surface heat flux and evaporation using large-scale parameters. Mon. Weather Rev. 100 (2), 81–92. https://doi.org/10.1175/1520-0493(1972)100<0081:OTAOSH>2.3.CO;2.

Richards, M., 2015. PyETo. In [Python package]. https://github.com/woodcrafty/PyETo. https://github.com/woodcrafty/PyETo.

Risacher, F., Fritz, B., 1991. Quaternary geochemical evolution of the salars of Uyuni and Coipasa, Central Altiplano, Bolivia. Chem. Geol. 90 (3), 211–231. https://doi.org/10.1016/0009-2541(91)90101-V.

Risacher, F., Fritz, B., 2009. Origin of salts and brine evolution of Bolivian and Chilean salars. Aquat. Geochem. 15, 123–157.

Risacher, F., Alonso, H., Salazar, C., 2003. The origin of brines and salts in Chilean salars: a hydrochemical review. Earth Sci. Rev. 63, 249–293.

Rissmann, C., Leybourne, M., Benn, C., Christenson, B., 2015. The origin of solutes within the groundwaters of a high Andean aquifer. Chem. Geol. 396, 164–181. https://doi.org/10.1016/j.chemgeo.2014.11.029.

Rossi, C., Bateson, L., Bayaraa, M., Butcher, A., Ford, J., Hughes, A., 2022. Framework for remote sensing and modelling of Lithium-brine deposit formation. Remote Sens. 14 (6).

Salisbury, M.J., Jicha, B.R., de Silva, S.L., Singer, B.S., Jiménez, N.C., Ort, M.H., 2011. 40Ar/39Ar chronostratigraphy of Altiplano-Puna volcanic complex ignimbrites reveals the development of a major magmatic province. GSA Bull. 123 (5–6), 821–840. https://doi.org/10.1130/B30280.1.

Schulzweida, U., 2020. CDO User Guide (Version 1.9.9). *Zenodo*. https://doi.org/10.5281/zenodo.4246983.

Szekely, G.J., Rizzo, M.L., 2005. Hierarchical clustering via joint between-within distances: extending Ward's minimum variance method. J. Classif. 22 (2), 151–183. https://doi.org/10.1007/s00357-005-0012-9.
Thornthwaite, C.W., 1948. An approach toward a rational classification of climate. Geogr. Rev. 38 (1), 55–94. https://doi.org/10.2307/210739.
Valiantzas, J.D., 2006. Simplified versions for the Penman evaporation equation using routine weather data. J. Hydrol. 331 (3–4), 690–702. https://doi.org/10.1016/j.jhydrol.2006.06.012.
WorldAtlas, 2020. Maps of South America. www.worldatlas.com.